Published in final edited form as:
Biomaterials. 2015 February ; 42: 144–150. doi:10.1016/j.biomaterials.2014.11.050.

Label-Free Imaging of Gelatin-Containing Hydrogel Scaffolds

Yajie Liang[a,b], **Amnon Bar-Shir**[a,b], **Xiaolei Song**[a,b], **Assaf A. Gilad**[a,b], **Piotr Walczak**[a,b], and **Jeff W.M. Bulte**[a,b,c,d,e,*]

[a]Russell H. Morgan Dept. of Radiology and Radiological Science, Division of MR Research, The Johns Hopkins University School of Medicine, Baltimore, MD 21205, USA

[b]Cellular Imaging Section and Vascular Biology Program, Institute for Cell Engineering, The Johns Hopkins University School of Medicine, Baltimore, MD 21205, USA

[c]Dept. of Chemical & Biomolecular Engineering, The Johns Hopkins University School of Medicine, Baltimore, MD 21205, USA

[d]Dept of Biomedical Engineering, The Johns Hopkins University School of Medicine, Baltimore, MD 21205, USA

[e]Dept of Oncology, The Johns Hopkins University School of Medicine, Baltimore, MD 21205, USA

Abstract

Composite hyaluronic acid (HA) hydrogels containing gelatin are used in regenerative medicine as tissue-mimicking scaffolds for improving stem cell survival. Once implanted, it is assumed that these biomaterials disintegrate over time, but at present there is no non-invasive imaging technique available with which such degradation can be directly monitored *in vivo*. We show here the potential of chemical exchange saturation transfer magnetic resonance imaging (CEST MRI) as a label-free non-invasive imaging technique to monitor dynamic changes in scaffold composition *in vivo*. The CEST properties of the three individual hydrogel components (HA, gelatin-GelinS, and polyethylene glycol diacrylate) were first measured *in vitro*. The complete hydrogel was then injected into the brain of immunodeficient *rag2*$^{-/-}$ mice and CEST MR images were obtained at day 1 and 7 post-transplantation. *In vitro*, GelinS gave the strongest CEST signal at 3.6 ppm offset from the water peak, originating from the amide protons present in gelatin. *In vivo*, a significant decrease in CEST signal was observed at 1 week post-implantation. These results were consistent with the biodegradation of the GelinS component, as validated by fluorescent microscopy of implanted hydrogels containing Alexa Fluor 488-labeled GelinS. Our label-free imaging approach should be useful for further development of hydrogel formulations with improved composition and stability.

*Corresponding Author: Jeff W.M. Bulte, Ph.D. Department of Radiology, The Johns Hopkins University School of Medicine, Broadway Research Building Rm 659, 733 N Broadway, Baltimore, MD 21205, Phone: 443-287-0996, Fax: 443-287-7945, jwmbulte@mri.jhu.edu.

1. Introduction

Hydrogels are hydrated, water-insoluble polymeric networks, cross-linked with water-soluble precursors [1], which are widely used to improve stem cell engraftment by providing a supportive three-dimensional tissue-mimicking microenvironment. A large number of *in vitro* and *in vivo* studies have demonstrated the feasibility of hydrogel-scaffolded cell transplantation for the regeneration or replacement of cartilage, cornea, liver, islets, and nerves [2]. Hyaluronic acid (HA), a major extracellular matrix component in the fetal mammalian brain, has been chemically modified in many ways to make a hydrogel scaffold with tunable properties [3]. Among these various modifications, thiol-modified HA hydrogels have favorable properties for use with cell transplantation, including excellent biocompatibility and ease of injection [4]. For the delivery of neural stem cells, reports have shown that an HA-based hydrogel composed of cross-linked thiol-modified heparin, gelatin, and HA significantly promoted the survival of neural progenitor cell (NPC) lines *in vitro* and *in vivo* after delivery into the ischemic stroke cavity in mouse brain [5], and improve the survival of several NPC lines in either immmunodeficient or immunocompetent animals [6].

Once transplanted, the microenvironment of the scaffolded, encapsulated cells may become subject to changes due to interactions between either stem cells and the gel or between the gel and the surrounding host tissue. Those interactions may cause changes in the physical and/or chemical properties of the scaffold, such as gel degradation or scaffold disassembly. It would be important to be able to monitor changes in scaffold composition non-invasively over time, as stem cells are particularly sensitive to changes in environmental cues, including the physical microenvironment and mechanical stress [7–10]. Indeed, a recent imaging study using Alexa Fluor-labeled HA reported that the clearance kinetics of biomaterials affects stem cell retention and therapeutic efficacy [11]. However, optical imaging is limited to small animal studies and does not directly report on the molecular structure of the hydrogel.

We investigated whether chemical exchange saturation transfer magnetic resonance imaging (CEST MRI) [12] is capable to observe dynamic changes in hydrogel scaffolds *in vivo*. CEST MRI is an emerging contrast mechanism for the detection of certain molecules with rapidly exchangeable protons that can be saturated with specific radiofrequency pulses [13]. Importantly, unlike optical imaging, MRI is ubiquitous in clinical imaging without limitations of tissue penetration depth. It has previously been shown that CEST MRI is able to monitor the viability of cells encapsulated in a hydrogel [14]. In this study, we hypothesized that the individual components of an injectable hydrogel (HA, gelatin-GelinS, and polyethylene glycol diacrylate) may have exchangeable protons that can provide CEST MRI contrast, and that this exchange would be dependent on the structure and integrity of the overall hydrogel.

2. Materials and Methods

2.1. Hydrogel preparation and fluorescent labeling

HA hydrogels (Hystem C, Glycosan BioSystems, Salt Lake City, UT) were prepared according to the manufacturer’s instructions by cross-linking thiol-modified sodium

hyaluronate (HA) and gelatin (GelinS, 300 g bloom) with polyethylene glycol diacrylate (PEGDA, M_w=3,400g/mole). HA, GelinS and PEGDA were dissolved in 0.1 M phosphate buffered saline (PBS) at the concentration of 10 mg/ml, 10 mg/ml and 20 mg/ml, respectively. The hydrogel was prepared at a volume ratio HA:GelinS:PEGDA=2:2:1. HA is the backbone of the hydrogel, which forms a network after crosslinking thiol-modified gelatin (GelinS) with PEGDA (Fig. 1a). The three gel components were mixed 20 minutes prior to use to allow for sufficient cross-linking [6]. Alexa Fluor 488-conjugated C5 maleimide (C5 dye, Invitrogen, Carlsbad, CA) was used to label either GelinS or HA. C5 dye was dissolved in degassed water, and the concentration of dye was measured using a Nanodrop (Thermo Fisher Scientific, Waltham, MA) in FITC dye mode. To determine optimal reaction conditions between maleimide and gelatin, different concentrations of maleimide were used to label GelinS and HA (as a control) before each was mixed with the other two non-labeled components. In these experiments, solutions of 160 μM, 16 μM, and 1.6 μM dye are referred to as high, medium, and low concentration dye solutions, respectively. Two μl of dye solution was added to 48 μl of either GelinS or HA solutions and incubated overnight at 4 °C. The hydrogel was then prepared by combining HA, GelinS, and PEGDA at the ratio mentioned above. Gelatin with 300 g bloom or 90–110 g bloom (Sigma, St. Louis, MO) was dissolved in 10 mM PBS at the same protein concentration as that of GelinS, as determined using a BCA protein assay kit (Thermo Fisher Scientific, Waltham, MA).

2.2. Measurements of hydrogel fluorescence intensity

Hydrogels with GelinS or HA labeled with Alexa Fluor 488-conjugated C5 maleimide were prepared at HA:GelinS:PEGDA=20:20:10 μl. A total of 50 μl of hydrogel was loaded into the wells of 96-well plates, and rinsed by PBS for 10 minutes before measuring the starting fluorescence intensity with a Multilabel reader (model 1420, Perkin Elmer, Waltham, MA, USA). The fluorescence intensity of the hydrogel was measured after collagenase (C*lostridium histolyticum*, type IV, Sigma, St. Louis, MO) treatment and again after rinsing with PBS for 10 minutes. To determine the natural decay of fluorescence from C5 maleimide-labeled hydrogel, 2 μl of hydrogel was loaded on the bottom of 24-well plates filled with 1 ml PBS, and the fluorescent intensity was measured for seven days. Images analysis of mean gray values was performed using Image J (NIH, Bethesda, MD).

2.3. Collagenase treatment and measurement of collagenase activity

GelinS was incubated with 0.1–100 U/ml C*lostridium histolyticum* collagenase type IV in 10 mM PBS overnight at 37°C. A precast 12% Tris-HCL gel (Bio-Rad, Hercules, CA, USA) was used for sodium dodecyl sulfate polyacrylamide gel electrophoresis (SDS-PAGE) of collagenase-treated and untreated gelatin. An EnzChek gelatinase/collagenase assay kit (Invitrogen, Carlsbad, CA) was used to measure collagenase activity in the supernatant of brain tissue. Brains were removed, manually homogenized in 10 mM PBS, pH=7.4, and then centrifuged at 16,000 g at 4°C for 20 minutes. C*lostridium histolyticum* collagenase was used as standard reference.

2.4. CEST MRI

In vitro CEST MRI was performed using an 11.7 T Bruker Avance spectrometer (Bruker, Billerica, MA) equipped with a 15 mm birdcage coil. Samples were loaded into microcapillaries oriented parallel to the z-axis of the magnet. Images were acquired with the following parameters: Slice thickness=1 mm, field of view (FOV)= 1.4x1.3 cm, matrix=128x64 (109x203 μm in plane resolution), RARE factor=16), repetition time/echo time (TR/TE)=6000/9.3 ms including a magnetization transfer (MT) module B_1=4.7 μT/4 s (−5 to +5 ppm, 0.2 ppm steps) around the water resonance (0 ppm). For B_0 corrections, the same parameters were used except TR=1500 ms, and B_1 =0.5 μT/0.5 s with sweeps from −2 to +2 ppm (step=0.1 ppm). *In vivo* CEST MRI was performed using a 9.4 T Bruker BioSpec (Bruker, Billerica, MA) scanner equipped with a 25 mm volume coil. The scan parameters were: slice of thickness=1 mm, FOV=1.5×1.5 cm, matrix=128x48 (117x312 μm in plane resolution, RARE factor=4, TR/TE=5000/16 ms, including an MT module B_1=3.0 μT/3 s (−4 to +4 ppm, 0.3 ppm steps) For B_0 corrections the same parameters were used except TR=1500 ms and B_1=0.5 μT/0.25 s with sweeps from −1.5 to +1.5 ppm (step=0.1 ppm). Data processing was performed using custom-written scripts in Matlab (MathWorks, Natick, MA).

2.5. Hydrogel implantation

All animal procedures were approved and conducted in accordance with our institutional guidelines for the use and care of laboratory animals. Injectable gel was prepared by mixing hydrogel components. Injection was initiated 25 minutes after mixing of the components. Immunodeficient, *rag2*$^{-/-}$ mice (n=4, male, 8–12 weeks old, Taconic Farms, Hudson, NY) were anesthetized with 2% isoflurane, shaved, and placed in a stereotaxic device (Stoelting Co. Wood Dale, IL). Three μl of complete hydrogel or hydrogel without GelinS was injected bilaterally into the striatum (AP=0; ML=2.0; DV=3.0 mm) at a rate of 0.5 μl/min, using a 31G microinjection needle attached to a 10 μl Hamilton syringe (Hamilton, Reno, NV). The needle was withdrawn slowly two minutes after the injection was complete. Mice were imaged at day 1 and day 7 after transplantation and thereafter processed for histology. In another set of experiments, hydrogels with either complete hydrogel or hydrogel without GelinS, both labeled with Alexa Fluor 488-conjugated C5 maleimide, were injected into the striatum of *rag2*$^{-/-}$ mice (n=4, male, 8–12 weeks old, Taconic Farms) using the same coordinates. Mice were sacrificed at day 1 or day 7, and the fluorescence intensity of the implanted hydrogel was quantified on cryosections as described below.

2.6. Histology and fluorescent microscopy

Animals were perfused with 4% paraformaldehyde and brains were dissected, cryoprocessed, and cut into 25-μm sections. For cresyl violet staining, sections of spinal cord or brain containing hydrogel implants were stained with 0.1% cresyl violet (Waldeck GmbH, Munster, Germany) solution for 10 minutes, dehydrated through a 70%, 95%, and 100% alcohol series, and then xylene. For hematoxylin and eosin (H&E, Sigma, St.Louis, MO) staining, sections were first stained with hematoxylin solution for 10 minutes. Coloring was developed in warm tap water for 10 minutes before staining with eosin for 1 minute, and sections were dehydrated as described above. Microscopic images were acquired with

an Olympus BX40 microscope (Olympus, Tokyo, Japan). For measurement hydrogel fluorescence intensity, images obtained at the same exposure time were quantitatively assessed using by calculating gray values using Image J software (NIH, Bethesda, MD).

2.7. Statistical Analysis

Statistical analysis was performed with an unpaired t-test (Mann-Whitney test) using prism 4.03 software (GraphPad, San Diego, CA). A paired Student's t-test was used for quantifying the CEST signal from the same animal at day 1 vs. day 7. Differences were considered statistically significant for $p<0.05$.

3. Results

3.1. CEST MRI properties of the individual hydrogel components

CEST imaging of the hydrogel phantoms was performed separately for each of the hydrogel components (HA, GelinS, and PEGDA). The highest CEST MRI contrast was obtained for GelinS, with high MTR asymmetry values at 1.8 and 3.6 ppm (Fig. 1b). HA also produced a strong CEST signal, with a peak at around 1 ppm (Fig. 1b). The contrast for PEGDA was negligible. As the signal of GelinS at 3.6 ppm is farther away from the water peak, it is more specific as compared to the HA peak. On the phantom CEST MR images, this resulted in a strong contrast for GelinS (Fig. 1c). After mixing the three components of the hydrogel (HA:GelinS:PEGDA=2:2:1), the overall hydrogel CEST contrast was lower due to a dilution effect for GelinS. These results indicate that GelinS can be effectively visualized with CEST MRI, and hence this component was chosen for further *in vivo* studies. As GelinS is the thiol-modified form of gelatin, we investigated whether the thiol modification could affect the CEST signal from gelatin. To this end, we included non-modified denatured gelatin from porcine skin with different bloom grades at the same protein concentration (12.5 mg/ml). The non-modified gelatin showed the same two signal peaks as that for GelinS, in a bloom grade-dependent manner (Fig. 1d). Thus, the CEST signal is gelatin-specific.

3.2. In vivo CEST MRI of implanted hydrogels

Complete hydrogel (HA:GelinS:PEGDA=2:2:1) or hydrogel without GelinS (HA: PEGDA=2:1) was bilaterally injected into the striatum. At one day after implantation, a significantly stronger CEST signal at 1.8 and 3.6 ppm could be observed at the GelinS site (Fig. 2a). Statistical analysis revealed that at both frequencies, there were significant differences in signal strength between the GelinS and non-GelinS hydrogels ($p<0.05$ at 1.8 ppm and $p<0.01$ at 3.6 ppm, Fig. 2b). As the 3.6 ppm data sets are farther from the water resonance frequency (0 ppm), it is a more specific marker for CEST contrast compared to 1.8 ppm. At day 7, the overall differences in signal became insignificant. There was a trend of decreasing CEST signal at 7 days, indicating a gradual decomposition of the hydrogel within the brain. However, cresyl violet staining demonstrated that the overall structure of the hydrogel was well-preserved (Fig. 2c).

3.3. Degradation of gelatin in vitro does not affect the CEST signal

Having evidence that the CEST contrast is primarily derived from gelatin and that there is a decay of CEST signal *in vivo*, we hypothesized that there must have been a substantial

change in the gelatin content or structure. Hence, we assessed the effect of degradation of gelatin on the CEST signal following incubation with collagenase. As shown by SDS-PAGE (Fig. 3a), non-digested GelinS was composed of different sizes of collagen segments. After digestion by collagenase, the resultant collagen strands were too small to be detected in the acrylamide gel. We found that 0.1 U/ml of collagenase was sufficient to completely digest GelinS by overnight incubation. Digested and undigested (control) GelinS samples were then processed for CEST MRI. Digestion of gelatin did not affect the CEST signal, with both peaks at 1.8 and 3.6 ppm remaining unaffected (Fig. 3b). These results indicate that the CEST signal from gelatin depends on the content of gelatin instead of its structure, and that the *in vivo* loss of CEST signal in implanted hydrogels is due to the physical clearance of gelatin from the hydrogel scaffold.

3.4. Measuring gelatin content in the hydrogel

To verify the loss of the gelatin component in the hydrogel, we first established an assay for gelatin content measurement by conjugating thiol-reactive, fluorescently tagged (Alexa Fluor 488 C5) maleimide to GelinS, which enables the correlation of fluorescence intensity with the content of gelatin in the hydrogel. For all three groups (high, medium, and low maleimide-fluorescent concentration), we found a significant increase in fluorescence intensity after incubation with collagenase (Fig. 4a, $p<0.01$), indicating dissociation of the fluorescent tag as a result of gelatin degradation within the hydrogel. Consistently, after rinsing with PBS, there was a significant decrease in fluorescence intensity ($p<0.01$). The fluorescence intensity in the hydrogel with labeled HA was stable in either the collagenase treated or non-treated groups (Fig. 4a). These data demonstrate that the fluorescence intensity in the hydrogel can serve as a marker for gelatin content, validating its further use for *in vivo* studies.

Next, we evaluated the natural decay of fluorescence from C5 maleimide-labeled gelatin to further evaluate the robustness of the fluorescence labeling method to report on gelatin levels. A natural decay of fluorescence occurred over time in the labeled hydrogel (Fig. 4b). The fluorescence intensity of HA-C5 hydrogel was higher than that of the GelinS-C5 hydrogel at day 1 ($p<0.05$), which can be explained by the larger number of binding sites on HA compared to GelinS (Fig. 1a). Quantification revealed an approximately 20% loss of original fluorescence intensity from each group over seven days (Fig. 4c). Incubation with 1 U/ml collagenase overnight greatly quenched the GelinS-C5 hydrogel ($p<0.01$ between fluorescence intensity from collagenase-treated and untreated GelinS-C5 hydrogel groups) but not the HA-C5 hydrogel groups (Fig. 4b). After seven days, the fluorescence intensity decreased to less than 20% of the initial value (Fig. 4c), in stark contrast to the approximately 80% fluorescence intensity measured for the non-collagease-treated group ($p<0.05$). The specific and significant loss of fluorescence in the collagenase-treated GelinS-C5 hydrogel further validates this experimental system. Altogether, these data confirm the validity of using C5-labeled maleimide labeling of gelatin as an indicator of the gelatin content within the hydrogel.

3.5. Decomposition of gelatin in the hydrogel scaffold in vivo

After implantation of hydrogels containing either C5-labeled GelinS or C5-labeled HA into mice brain, a significant decrease in the fluorescent signal was found for the labeled gelatin hydrogel for day 7 as compared to day 1 (Fig. 5a, $p<0.05$). Quantification of the fluorescence intensity revealed an approximately 60% loss of fluorescence in the GelinS labeled group, significantly higher than the loss observed in the HA-C5 hydrogel group (Fig. 5b, $p<0.05$). This is consistent with our imaging findings that the gelatin is disintegrating and cleared from the hydrogel over time. We also found a decrease of fluorescence intensity in the HA-C5 hydrogel group, albeit to a much lesser extent (Fig. 5a). To further substantiate possible decomposition of gelatin in the hydrogel, we measured the activity of collagenase in the brain using commercially available collagenase as a reference. The concentration of collagenase in the normal *rag2*$^{-/-}$ striatum was calculated to be around 10 to 15 μU/ml (Fig. 5c).

4. Discussion

With the rapid development of novel biomaterials and hydrogel scaffolds aimed to enhance the efficacy of stem cell therapy, there is an urgent need for non-invasive imaging methods that can report on the fate of the implanted scaffolds, in particular if and for how long they stay intact or decompose, and how this may affect the survival and function of scaffolded stem cells. We describe here, for the first time, a label-free non-invasive imaging technique that can report on hydrogel decomposition in a clinically translatable fashion.

CEST MRI is a relatively new imaging approach in which exogenous or endogenous compounds, containing exchangeable protons at specific frequencies, are selectively saturated at specific frequencies to prevent them from contributing to the MRI signal. After transfer of their saturation to bulk water, from which the proton MRI signal is derived, the water signal is reduced; hence these exchangeable protons are detected indirectly. CEST imaging is now being recognized as an emerging technique for molecular and cellular MR imaging: it can be used to detect MRI reporter genes [15–17], enzyme activity [18], pH changes associated with cell death [14], and the occurrence of an immune response against foreign body materials [19].

In this study, we found that GelinS, a denatured type 1 collagen derived from porcine skin, provides good CEST contrast at 1.8 and 3.6 ppm (Fig. 1c), and can be detected *in vivo* (Fig. 2a). The putative source of the CEST signal are the amide groups on type 1 collagen as unmodified gelatin produced a similar pattern of CEST contrast (Fig. 1d), and amide protons are known to produce specific CEST contrast at 3.6 ppm. [20]. The 1.8 ppm is derived from arginine protons, with gelatin containing 8–9% arginine [21].

We found a significant decrease in CEST contrast from the implanted hydrogel in mice brain over seven days (Figs. 2a,b). According to the in vitro phantom study (Fig. 1), the CEST contrast is primarily derived from gelatin, and therefore the decay in those signals strongly suggests that it is the gelatin component within the scaffold undergoing substantial changes *in vivo* at Day 7. We hypothesized that the disappearance of the CEST signal from the gelatin could be correlated with the integrity of the physical scaffold network of gelatin

in that a decrease in CEST signal would result from degradation of the gelatin network into shorter segments, even though gelatin may not necessarily be dissociated from the hydrogel scaffold. To test this hypothesis, we performed *in vitro* experiments on gelatin with and without collagenase digestion. To the contrary, we found that the two peaks of CEST signal at 1.8 and 3.6 ppm did not change after gelatin digestion (Fig. 3b), indicating that the length of the gelatin molecules does not affect the CEST signal. Hence, the decreased CEST contrast of the hydrogel must be a consequence of the physical clearance or leakage of the gelatin components from the hydrogel scaffold network.

The ideal method to verify the clearance of gelatin from the hydrogel would be to perform direct anti-gelatin specific immunostaining. However, several sources of antibodies against denatured collagen 1 from porcine skin failed to specifically stain the gelatin components in the hydrogel (data not shown), possibly as a result from a mixture of molecules of different sizes and the linearized antigen epitopes that are not specific to denatured gelatin. We therefore attempted an indirect method, i.e., the conjugation of a fluorescent dye to gelatin to detect its presence by fluorescence microscopy. In fact, the most common way to detect collagenase activity is the use of a fluorescently labeled substrate (gelatin) [22]. In our case, the gelatin content was immobilized in a hydrogel scaffold, making it applicable for solid phase-based assays.

Our finding that collagenase activity interacts with gelatin in the implanted hydrogel raises two questions: 1) What is the source of this collagenase activity, and 2) What are the implications for further optimization of hydrogel-based scaffold cell therapy? Members of the matrix metalloproteinase (MMP) family are the most likely sources of endogenous collagenase activity. In the brain, MMPs are secreted by microglia, astrocytes, and endothelial cells for extracellular matrix remodeling [23]. MMP-1 and MMP-2 have been reported to possess type I collagenase activity under many conditions [24–26], with most attention on their role as a type IV collagenase in cell invasion across the basement membrane. It is also possible that other MMPs may be involved due to the local neuroinflammation induced by a hydrogel [27]. As the addition of gelatin to the HA hydrogel is intended to improve the survival of scaffolded cells, the degradation of gelatin may impair its pro-survival ability, leading to only short-term neuroprotection conferred by this hydrogel[6]. In this case, it is preferable to modify the gelatin in such a way that it will not be degraded by MMPs, or to apply inhibitors of MMPs [28]. In this context, our label-free CEST MRI method may be uniquely suited to investigate future improvements in hydrogel scaffold composition and materials.

This imaging technique can furthermore also be combined with direct cell imaging techniques, e.g. bioluminescent imaging, to investigate the correlation between hydrogel decomposition and hydrogel-scaffolded cell survival [6]. Alternatively, the therapeutic stem cells could be labeled with a superparamagnetic iron oxide MR contrast agent before scaffolding them [29], in order to provide concurrent cell-induced hypointense vs. scaffold-induced CEST contrast [30].

5. Conclusions

We identified gelatin, a widely used component in tissue hydrogels, as a chemical structure that provides a strong CEST MRI contrast at 1.8 and 3.6 ppm. As the gelatin CEST contrast is unaffected by direct collagenase digestion, the changes in contrast are a result from local gel decomposition and tissue clearance. Our label-free method allows monitoring of the fate of implanted scaffolds *in vivo*, which should prove useful for the further use of hydrogel biomaterials in regenerative medicine.

Acknowledgements

This work was supported by 2R01 NS045062. We thank Mary McAllister for editorial assistance.

References

1. Elisseeff J. Hydrogels: structure starts to gel. Nat Mater. 2008; 7:271–273. [PubMed: 18354410]
2. Wang C, Varshney RR, Wang DA. Therapeutic cell delivery and fate control in hydrogels and hydrogel hybrids. Adv Drug Deliv Rev. 2010; 62:699–710. [PubMed: 20138940]
3. Burdick JA, Prestwich GD. Hyaluronic acid hydrogels for biomedical applications. Adv Mater. 2011; 23:H41–H56. [PubMed: 21394792]
4. Shu XZ, Ahmad S, Liu Y, Prestwich GD. Synthesis and evaluation of injectable, in situ crosslinkable synthetic extracellular matrices for tissue engineering. J Biomed Mater Res A. 2006; 79:902–912. [PubMed: 16941590]
5. Zhong J, Chan A, Morad L, Kornblum HI, Fan G, Carmichael ST. Hydrogel matrix to support stem cell survival after brain transplantation in stroke. Neurorehabil Neural Repair. 2010; 24:636–644. [PubMed: 20424193]
6. Liang Y, Walczak P, Bulte JW. The survival of engrafted neural stem cells within hyaluronic acid hydrogels. Biomaterials. 2013; 34:5521–5529. [PubMed: 23623429]
7. Engler AJ, Sen S, Sweeney HL, Discher DE. Matrix elasticity directs stem cell lineage specification. Cell. 2006; 126:677–689. [PubMed: 16923388]
8. Seidlits SK, Khaing ZZ, Petersen RR, Nickels JD, Vanscoy JE, Shear JB, et al. The effects of hyaluronic acid hydrogels with tunable mechanical properties on neural progenitor cell differentiation. Biomaterials. 2010; 31:3930–3940. [PubMed: 20171731]
9. Alsberg E, von Recum HA, Mahoney MJ. Environmental cues to guide stem cell fate decision for tissue engineering applications. Expert Opin Biol Ther. 2006; 6:847–866. [PubMed: 16918253]
10. Chowdhury F, Na S, Li D, Poh YC, Tanaka TS, Wang F, et al. Material properties of the cell dictate stress-induced spreading and differentiation in embryonic stem cells. Nat Mater. 2010; 9:82–88. [PubMed: 19838182]
11. Lai CY, Wu PJ, Roffler SR, Lee ST, Hwang SM, Wang SS, et al. Clearance kinetics of biomaterials affects stem cell retention and therapeutic efficacy. Biomacromolecules. 2014; 15:564–573. [PubMed: 24372561]
12. Ward KM, Aletras AH, Balaban RS. A new class of contrast agents for MRI based on proton chemical exchange dependent saturation transfer (CEST). J Magn Reson. 2000; 143:79–87. [PubMed: 10698648]
13. van Zijl PC, Yadav NN. Chemical exchange saturation transfer (CEST): what is in a name and what isn't? Magn Reson Med. 2011; 65:927–948. [PubMed: 21337419]
14. Chan KW, Liu G, Song X, Kim H, Yu T, Arifin DR, et al. MRI-detectable pH nanosensors incorporated into hydrogels for in vivo sensing of transplanted-cell viability. Nat Mater. 2013; 12:268–275. [PubMed: 23353626]
15. Gilad AA, McMahon MT, Walczak P, Winnard PT Jr, Raman V, van Laarhoven HW, et al. Artificial reporter gene providing MRI contrast based on proton exchange. Nat Biotechnol. 2007; 25:217–219. [PubMed: 17259977]

16. Airan RD, Bar-Shir A, Liu G, Pelled G, McMahon MT, van Zijl PC, et al. MRI biosensor for protein kinase A encoded by a single synthetic gene. Magn Reson Med. 2012; 68:1919–1923. [PubMed: 23023588]
17. Bar-Shir A, Liu G, Chan KW, Oskolkov N, Song X, Yadav NN, et al. Human protamine-1 as an MRI reporter gene based on chemical exchange. ACS chemical biology. 2014; 9:134–138. [PubMed: 24138139]
18. Liu G, Liang Y, Bar-Shir A, Chan KW, Galpoththawela CS, Bernard SM, et al. Monitoring enzyme activity using a diamagnetic chemical exchange saturation transfer magnetic resonance imaging contrast agent. J Am Chem Soc. 2011; 133:16326–16329. [PubMed: 21919523]
19. Chan KW, Liu G, van Zijl PC, Bulte JW, McMahon MT. Magnetization transfer contrast MRI for non-invasive assessment of innate and adaptive immune responses against alginate-encapsulated cells. Biomaterials. 2014; 35:7811–7818. [PubMed: 24930848]
20. Goffeney N, Bulte JW, Duyn J, Bryant LH Jr, van Zijl PC. Sensitive NMR detection of cationic-polymer-based gene delivery systems using saturation transfer via proton exchange. J Am Chem Soc. 2001; 123:8628–8629. [PubMed: 11525684]
21. Eastoe JE. The amino acid composition of mammalian collagen and gelatin. The Biochemical journal. 1955; 61:589–600. [PubMed: 13276342]
22. Sugiyama K, Yamamoto K, Kamata O, Katsuda N. A simple and rapid assay for collagenase activity using fluorescence-labeled substrate. Kurume Med J. 1980; 27:63–69. [PubMed: 6253726]
23. Mun-Bryce S, Rosenberg GA. Matrix metalloproteinases in cerebrovascular disease. J Cereb Blood Flow Metab. 1998; 18:1163–1172. [PubMed: 9809504]
24. Deryugina EI, Bourdon MA, Reisfeld RA, Strongin A. Remodeling of collagen matrix by human tumor cells requires activation and cell surface association of matrix metalloproteinase-2. Cancer Res. 1998; 58:3743–3750. [PubMed: 9721888]
25. Haas TL, Davis SJ, Madri JA. Three-dimensional type I collagen lattices induce coordinate expression of matrix metalloproteinases MT1-MMP and MMP-2 in microvascular endothelial cells. J Biol Chem. 1998; 273:3604–3610. [PubMed: 9452488]
26. Fukuda Y, Ishizaki M, Kudoh S, Kitaichi M, Yamanaka N. Localization of matrix metalloproteinases-1, -2, and -9 and tissue inhibitor of metalloproteinase-2 in interstitial lung diseases. Lab Invest. 1998; 78:687–698. [PubMed: 9645759]
27. Candelario-Jalil E, Yang Y, Rosenberg GA. Diverse roles of matrix metalloproteinases and tissue inhibitors of metalloproteinases in neuroinflammation and cerebral ischemia. Neuroscience. 2009; 158:983–994. [PubMed: 18621108]
28. Wang X, Li KF, Adams E, Van Schepdael A. Matrix metalloproteinase inhibitors: a review on bioanalytical methods, pharmacokinetics and metabolism. Curr Drug Metab. 2011; 12:395–410. [PubMed: 21395524]
29. Srivastava AK, Bulte JW. Seeing stem cells at work in vivo. Stem cell reviews. 2014; 10:127–144. [PubMed: 23975604]
30. Gilad AA, van Laarhoven HW, McMahon MT, Walczak P, Heerschap A, Neeman M, et al. Feasibility of concurrent dual contrast enhancement using CEST contrast agents and superparamagnetic iron oxide particles. Magn Reson Med. 2009; 61:970–974. [PubMed: 19189296]

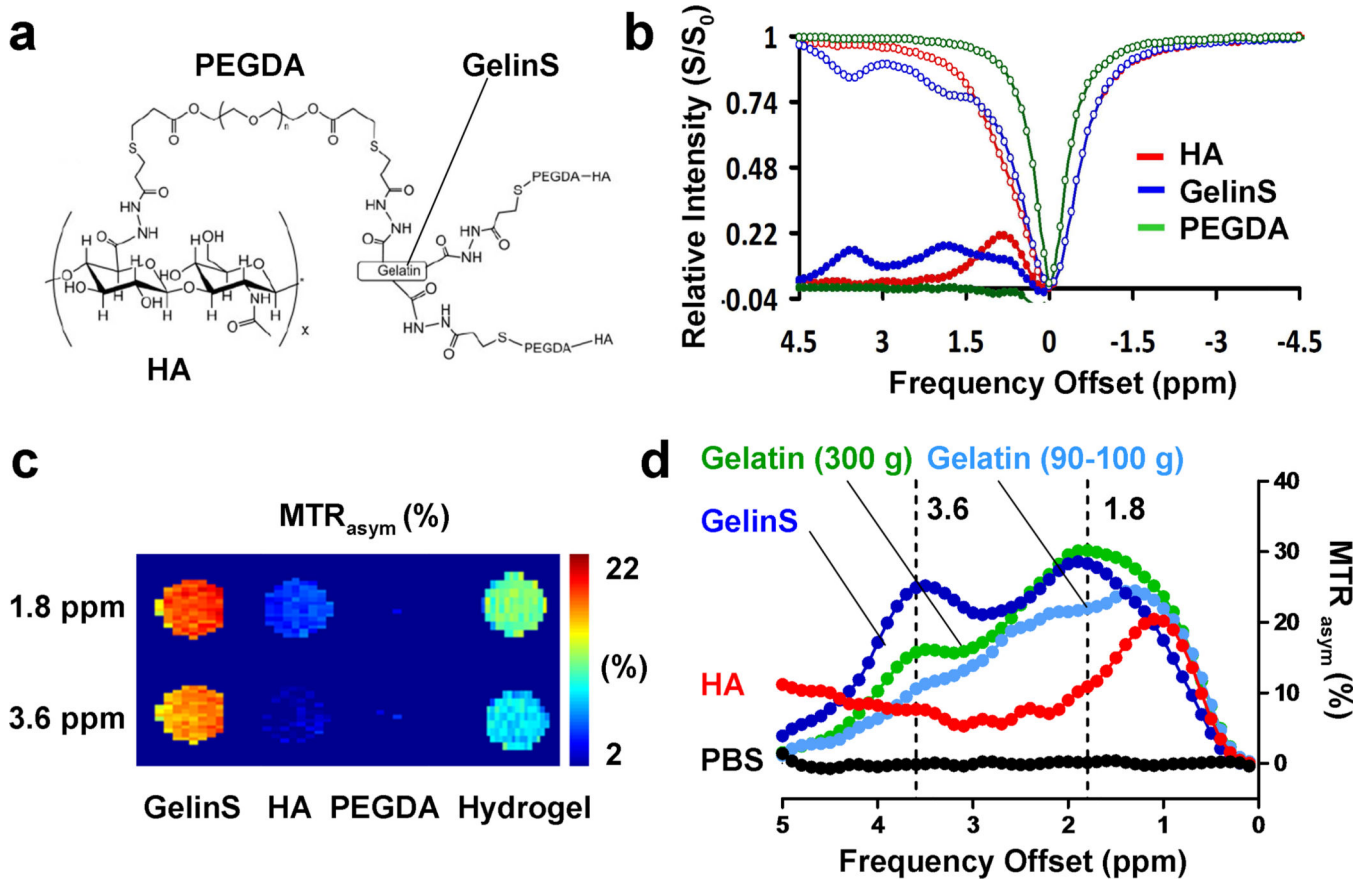

Fig. 1.

In vitro CEST MRI of individual HA hydrogel components. (a) Chemical structure of the entire cross-linked hydrogel. (b) Z-spectrum and MTR asymmetry map of the three individual hydrogel components (red=GelinS, blue=HA, green=PEGDA). (c) CEST contrast of the three individual hydrogel components at 1.8 and 3.6 ppm. (d) CEST contrast of different compounds: HA, GelinS, 300 g bloom gelatin, 90–110 g bloom gelatin), and PBS (control).

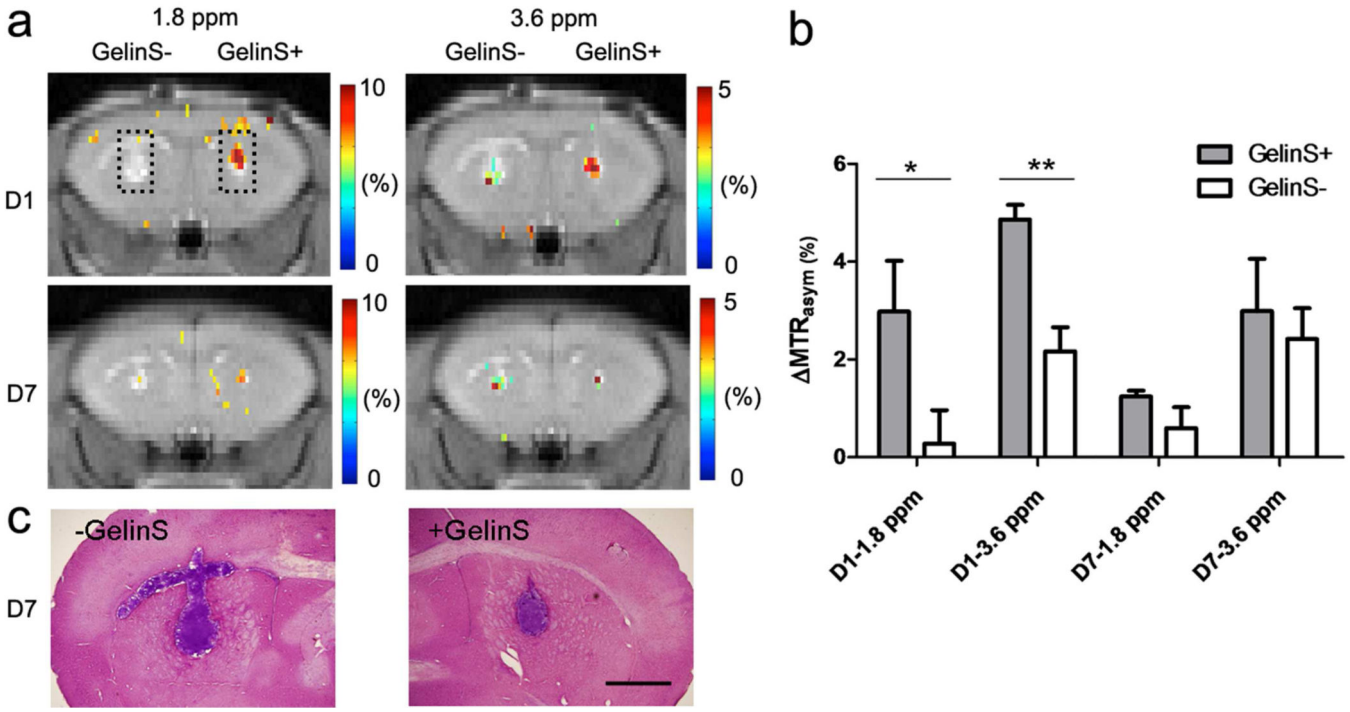

Fig. 2.

In vivo CEST MRI of implanted hydrogels. (a) CEST MR images were acquired at 1.8 ppm and 3.6 ppm for HA hydrogel implants with and without GelinS at day 1 and day 7 post-injection. Hydrogel implants are indicated by dashed squares. (b) Quantification of CEST contrast in the hydrogel implants. Values shown are means ±SEM. (n=4). (c) Histological assessment at day 7 after transplantation using H&E-cresyl violet staining, in which the scaffold appears purple. Scale bar=1 mm.

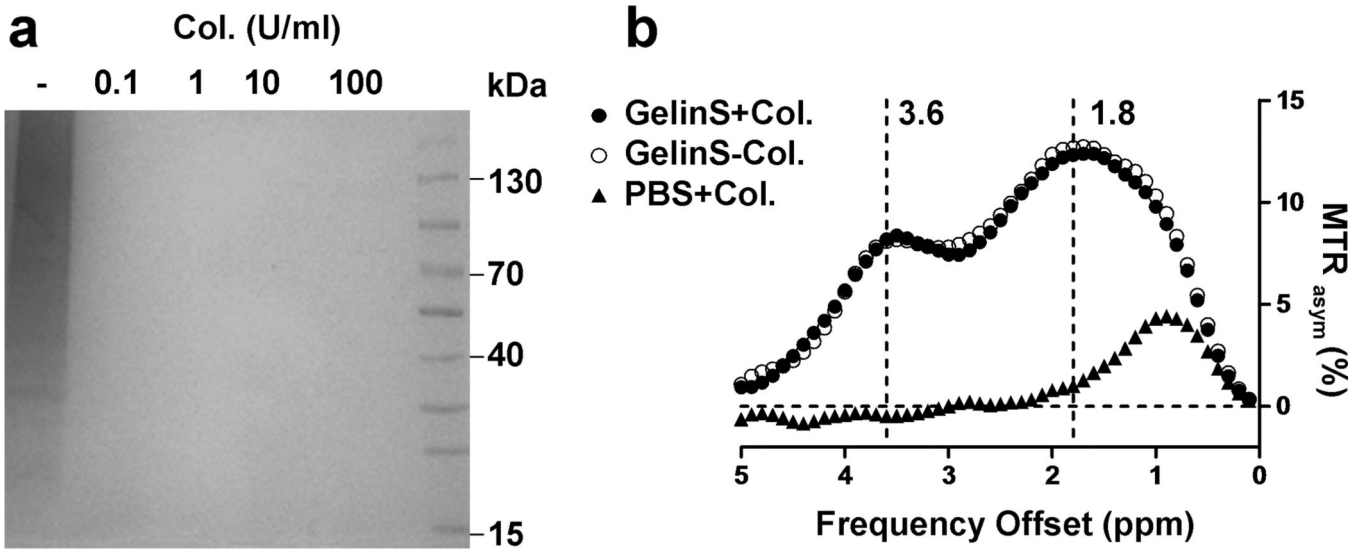

Fig. 3.

Effect of gelatin decomposition on CEST contrast of GelinS. (a) GelinS was digested with overnight collagenase (Col) incubation at different concentrations (0, 0.1, 1, 10, and 100 U/ml) and then run by SDS-PAGE. (b) CEST MRI contrast of digested (GelinS+Col., 1 U/ml) and non-digested GelinS (GelinS-Col.) samples. As control, the same amount of collagenase without GelinS was measured (PBS+Col.).

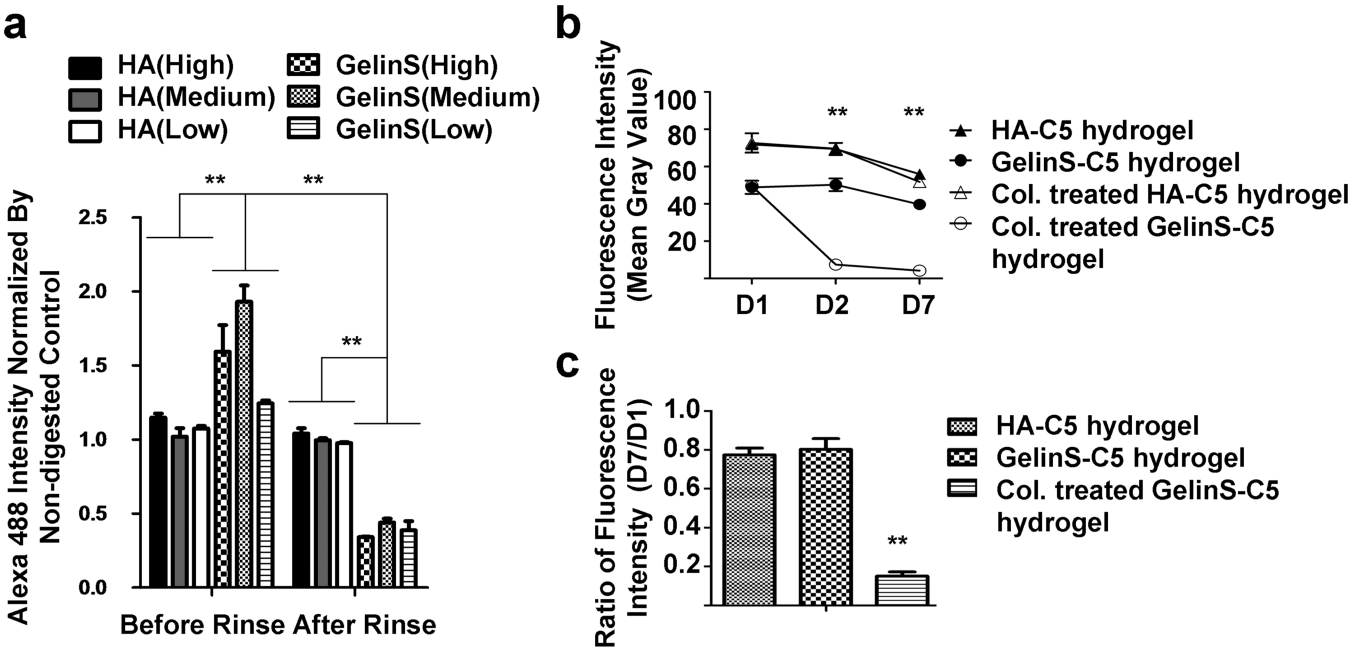

Fig. 4.

Quantification of GelinS content in the hydrogel. (a) Alexa Fluor 488 C5-maleimide was reacted with GelinS or HA at low, medium, and high concentrations before synthesizing the complete hydrogel, which was then incubated with collagenase (1 U/ml) to achieve gelatin degradation. Fluorescence intensity was read before and after rinsing with PBS. (b) GelinS-C5 or HA-C5 hydrogels were incubated at 37°C for a week with and without the presence of collagenase (Col., 1 U/ml), and changes in fluorescence intensity were measured. (c) Measured fluorescence intensity at day 7, normalized to day 1 (D7/D1). Significance level was set at $^{**}p<0.01$. Values shown are means ±SEM (n=5).

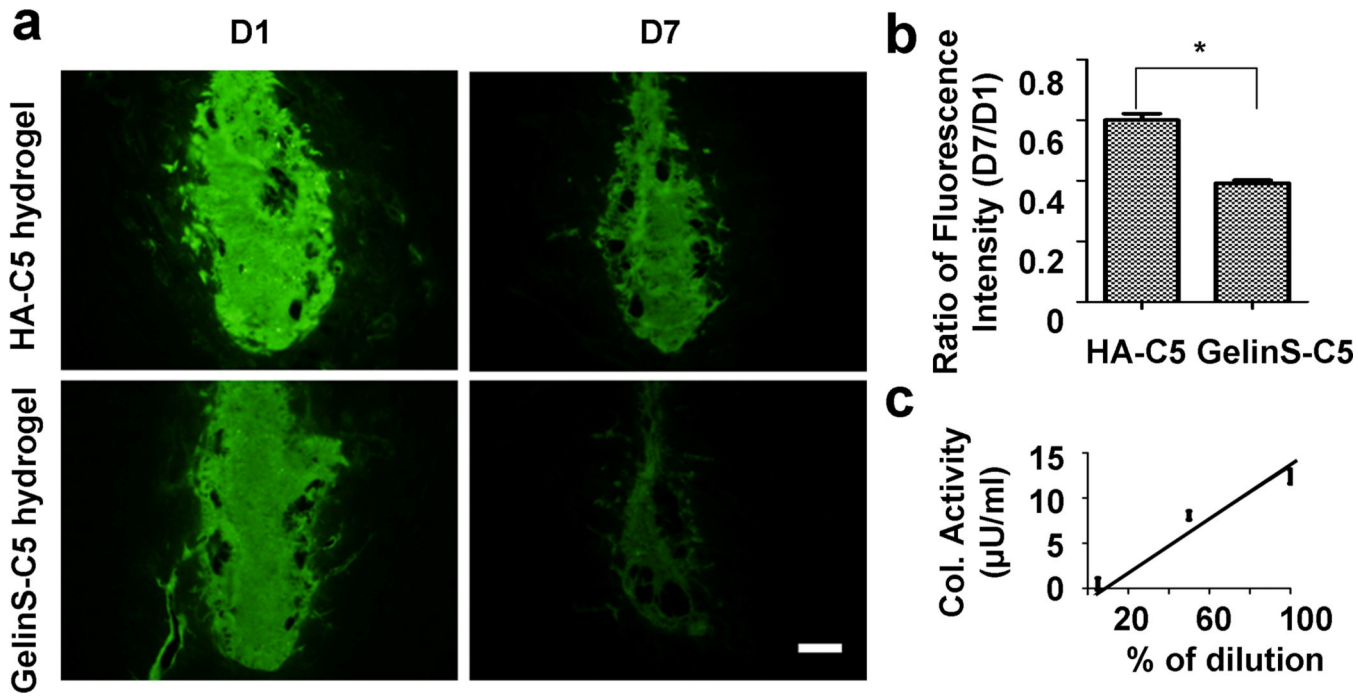

Fig. 5.

Decomposition of gelatin *in vivo*. (a) Hydrogels with either HA-C5 or GelinS-C5 conjugated to Alexa Fluor 488 were injected into mice brain, and the fluorescence intensity of the hydrogel was measured at day 1 or day 7. Scale bar=200 μm. (b) Measured fluorescence intensity at day 7, normalized to day 1 (D7/D1). Significance level was set at $*p<0.05$. Values shown are means ±SEM (n=4). (c) Measurement of collagenase activity in brain extracts of *rag2*$^{-/-}$ mice (n=4).